Authors' Response to Comments from anonymous referee #2

Black, italic: Referee's comments

Blue: Author's reply

Red: Changes in the original discussion paper

Xi et al. present a new airborne imaging DOAS instrument and results of the first demonstration flight. The results are encouraging and data might be interesting for further analysis such as satellite validation, emission estimates or model comparison. The paper fits very well in the context of AMT. However at some points more details might be required by the reader. Most of them are not critical but require an update of the manuscript.

First, we appreciate the overall positive response of the referee and we would like to thank for his constructive comments and helpful suggestions on the manuscript. As described below, we have modified the manuscript according to suggestions and provided clarifications where necessary.

1. Through out the manuscript the authors should take care to distinguish between total and tropospheric vertical columns - in most cases the tropospheric vertical column or to be more precise the column below the flight altitude is meant e.g. l 167.

In this manuscript, the NO_2 vertical columns we calculated are tropospheric vertical columns. We added necessary clarification throughout the manuscript. For example, we changed the title of the manuscript to 'The first high-resolution tropospheric NO2 observations from the Ultraviolet Visible Hyperspectral Imaing Spectrometer (UVHIS)'.

2. The NO2 fit shown in figure 4 has some residual structures, which might be noise but might also be caused by a systematic issue. The instrument was carefully calibrated before the measurements. The wavelength calibration is used only as apriori for the QDOAS software - which is certainly necessary. The slit function shape that can be extracted from the measurements using the Mercury-Argon lamp but are not shown or mentioned. Instead a symmetric Gaussian slit function is assumed in the DOAS analysis. The width of the slit function varies significantly within the fitting window (figure 3) - maybe the shape does so as well? I suggest adding at least a figure of the measured slit function for the extreme viewing directions (left, centre and right) including the Gaussian fit.

We added a figure of measured slit functions at 450.504 nm for 9 viewing angles (-20°, -15°, -10°, -5°, 0°, 5°, 10°, 15°, 20°), and the respective Gaussian fit results. These Gaussian fit results suggest that a symmetric Gaussian function is a reasonable assumption for slit shape in all viewing directions.
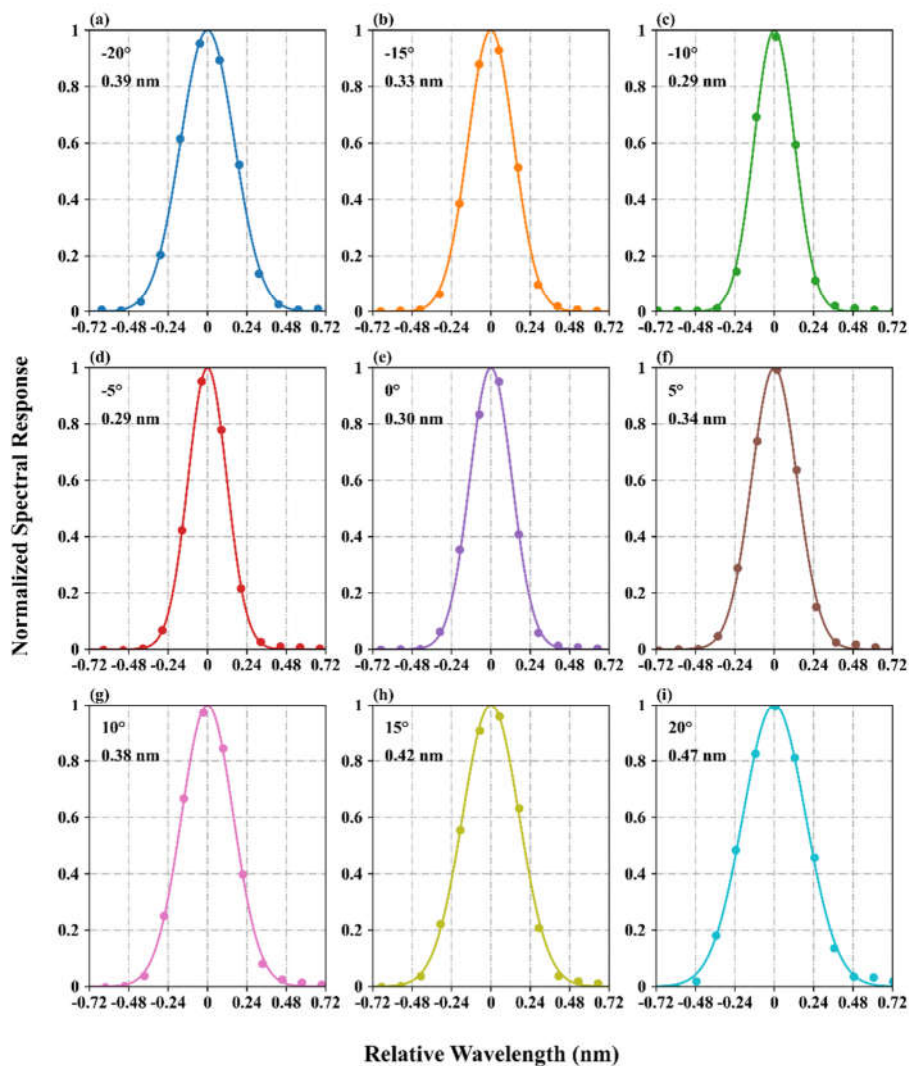
Figure 2. Measured slit functions (dots) at 450.504 nm and retrieved slit function shapes (lines) using a symmetric Gaussian function for 9 viewing angles.

The preflight wavelength calibration was also performed in the laboratory, using a mercury–argon lamp and a tunable laser as light sources. We model the slit function of UVHIS using a symmetric Gaussian function. Spectral registration and slit function calibration are achieved by least square fitting of characteristic lines in collected spectra. Table 2 lists the retrieved full-width at half maximums (FWHMs) for channel 3. Figure 2 shows the measured slit functions at 450.504 nm for 9 viewing angles (-20°, -15°, -10°, -5°, 0°, 5°, 10°, 15°, 20°), and respective retrieved slit function shapes using a symmetric Gaussian function. These Gaussian fit results suggest that a symmetric Gaussian function is a reasonable assumption for slit shape in all viewing directions.

3. The observations partly overlap as the distance between the parallel flighttracks was 1.5 km and the swath width is 2.2 km. How good do the observed tropospheric NO2 columns agree in the overlapping regions, does this depend on the flight direction and time, according to figure 2 some parts of the flight track were covered at least twice.

Indeed, several fight lines are repeated in the northern part of flight area, but the spectral data of UVHIS are not recorded because of misoperation. Only spectral data of the flight lines over the steel factory are recorded, and the pass time of aircraft is 13:26 and 14:57 respectively. We added a paragraph and a figure to discuss this in detail.
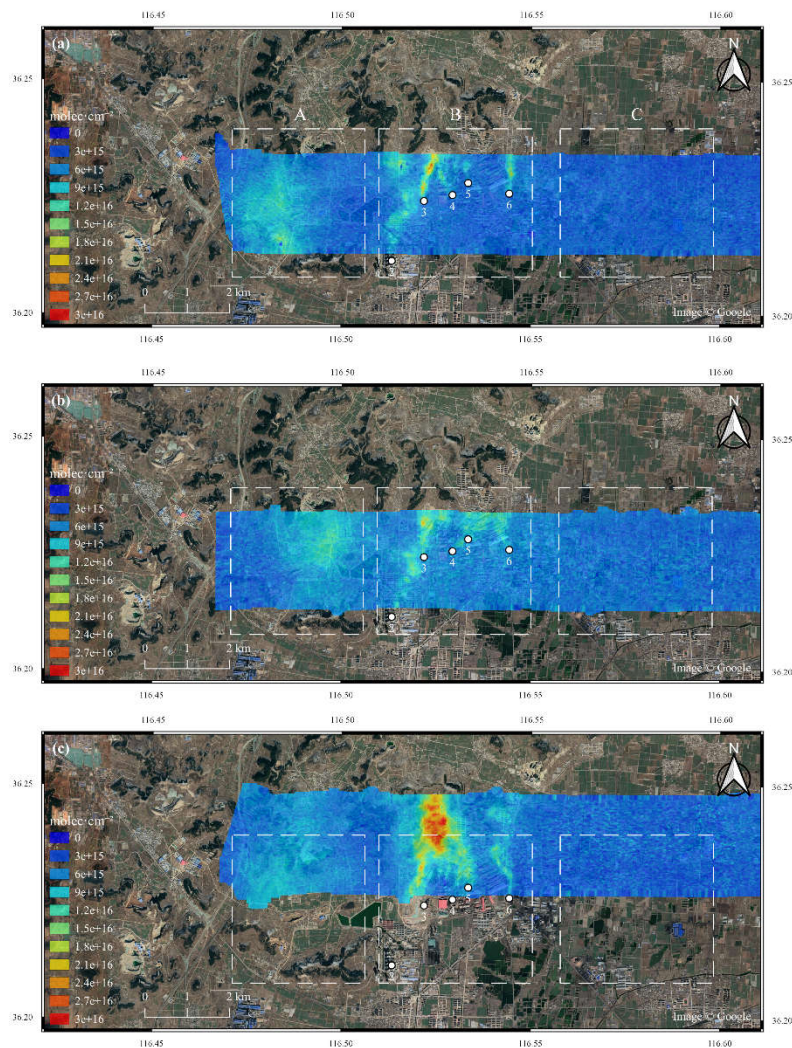

Figure 12. Three flight lines that pass through the steel factory, at local time 13:26 (a), 13:32 (c), and 14:57 (b). Panel (a) and (b) represent flight lines that cover the same area with a 1.5 hour time gap, panel (a) and (c) represent adjacent flight lines with a 6 minutes time gap.

Due to temporal discontinuity of flight lines and dynamic characteristics of NO$_2$ field, artefacts can be observed between adjacent flight lines. Figure 12 shows three flight lines that pass through the steel factory, at local time 13:26 (a), 13:32 (c), and 14:57 (b). Panel (a) and (b) represent flight lines that cover the same area with a 1.5 hour time gap, panel (a) and (c) represent adjacent flight lines with a 6 minutes time gap. These flight lines can be divided into three regions: region A covers no NO$_2$ source but is affected by carbon factories about 3 km away; region B covers the steel factory as dominant NO$_2$ source; region C covers no NO$_2$ source and is not affected by other sources. Compared to region B, there is a large temporal variety of NO$_2$ VCDs in region A between three flight lines. Region C is temporally consistent with relatively low NO$_2$ columns. From these observations it may be concluded that largest temporal variability could occur where there is no local NO$_2$ source but is down-wind of other sources, especially when wind direction is changing.

4. The error given here is not the fitting error but the total error of the VCD - even if the fitting error ~4.8 x 10^15 molec/cm^2 is probably the dominant contribution.

Corrected.

5. The instrument was build for airborne measurements in the troposphere, however the spectral range encompasses the deep UV from 200-276 nm in channel 1, I am afraid the intensity in this channel will be very low. Through out the manuscript the data from the channels 1 and 2 are not shown nor used. Airborne measurements often face the problem of the instruments being too heavy, therefore I am surprised to read that the instruments has a channel 1 that seems not very useful. Maybe the authors can briefly comment about the potential use of the channels 1 and 2, or the former use in a different instrument. For channel 2 I can think of the retrieval of SO2 or HCHO, both would interesting for the presented study but may require a more detailed analysis.

The UVHIS is part of a full spectral multimodal airborne imaging spectrometer. Our works only involve the channel 2 and 3 for trace gas measurements. In future works, we will present the retrieval results of SO$_2$ or HCHO based on measurements of channel 2. For channel 1 that covers deep UV spectral range, it is beyond our scope of work, and it may be used for wildfire or other artificial UV light source detection.

6. The figure of the instrument (figure 1) is a bit confusing it might be clearer if the authors reduce the number of light beams. It seems that part of the "red" light beam originating from the "top" is blocked by the convex grating, I suppose this is not the case, maybe because it is shifted relative to the drawing plane in the third dimension? Does second perspective view helps to explain more clearly? A radiometric calibration was performed as well as a spectral calibration. However, it seems the data form the radiometric calibration were not used it might be interesting to see the calibrated intensity in comparison to the LANDSAT 8 albedo (figure 7).

We replot Figure 1 with less number of light beams in the manuscript, also another figure added here would help to explain the structure more clearly.

For better comparison with surface reflectance and AMF, we added a panel in Figure 9 of radiance measurements from UVHIS. It is obvious that all panels share a same spatial distribution. However, some small differences can be observed due to time offset and spatial resolution difference.

1. Telecentric fore-optics
2. Filter and slit
3. Concave mirror
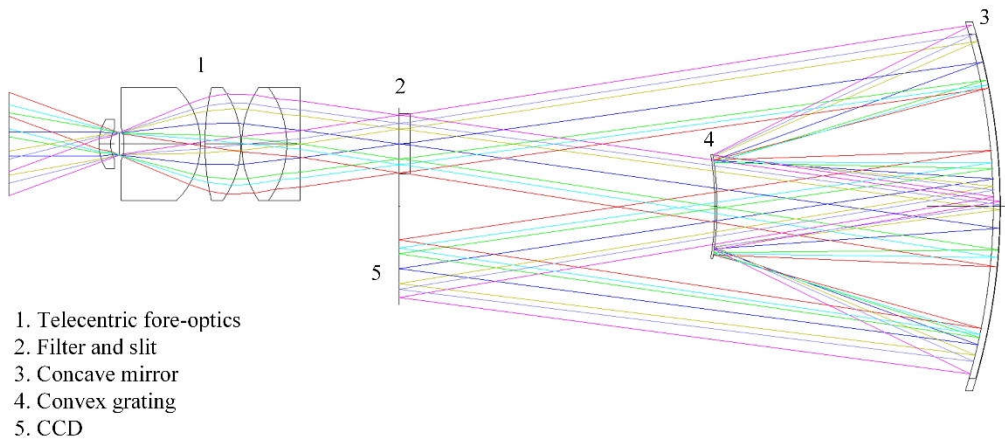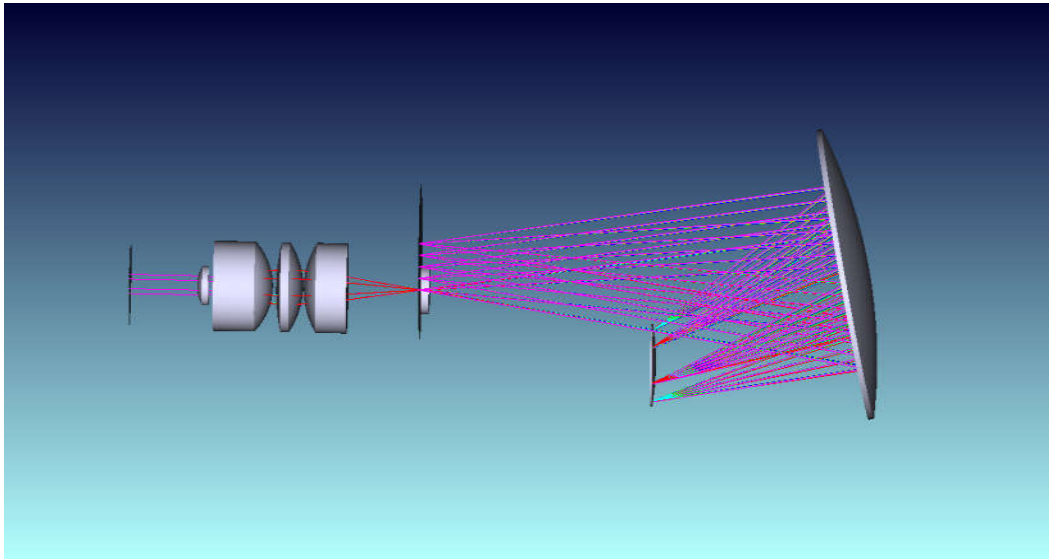4. Convex grating
5. CCD

Figure 1. Optical layout of the UVHIS channel 3. Optical design of channel 1 and channel 2 is similar.
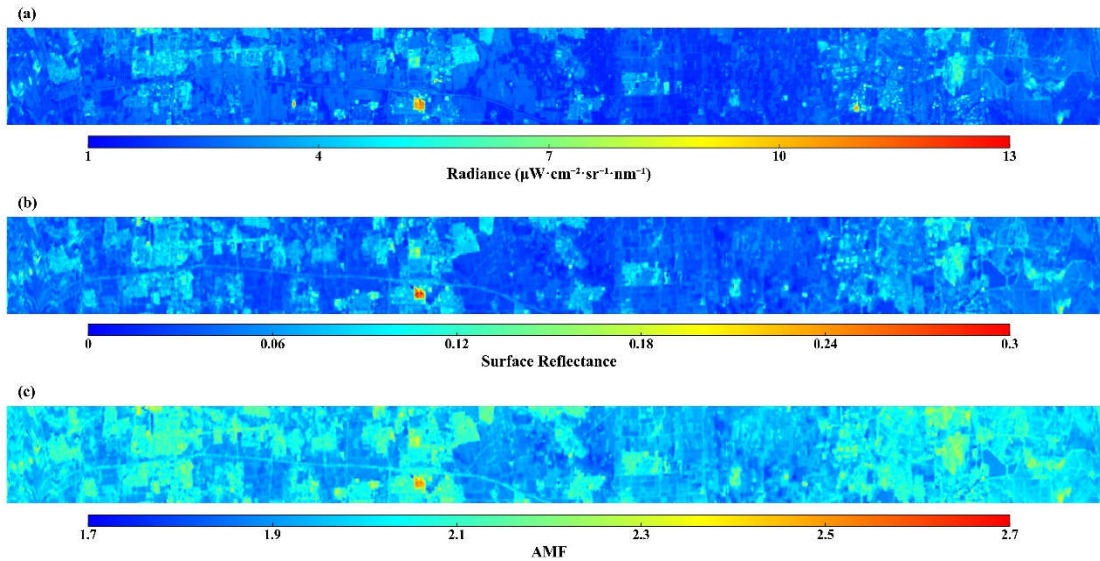
Figure 9. (a) UVHIS Measured radiance; (b) Landsat 8 Surface reflectance, (c) computed AMFs, for one flight line of the Feicheng data set. A strong dependency of the AMF on the surface reflectance can be observed.

7. Parts of CCD are blocked to control offset and dark current which is a good idea if this part of the CCD can not be used for real observation. However in section 4 the well established pre-flight dark current and offset measurements are used and the dark measurements at the edges of the CCD are not mentioned.

Both pixels at left and right edge on the CCD detector are blocked to monitor dark current. During the flight, signals from these pixels are very stable due to the temperature stability of the instrument. For dark current correction, we prefer to use pre-flight dark current measurements for the entire CCD detector because the dark measurements at the edges of the CCD only cover a small part of the CCD.

8. For non Chinese readers some more details about the measurement area might be nice to have. Can you add a map of China indicating where the city of Feiching is and in the context of the paper a satellite observation of NO2 for the day or season might be included as well.

Feicheng is a county-level city in Shandong province, China, about 410 km away from Beijing. The flight area is located on the south bank of the Yellow River, at the western foot of Mount Tai. We added a figure of TROPOMI NO_2 tropospheric observation on 23 June, 2018, with the background Google map and the location of Feicheng.
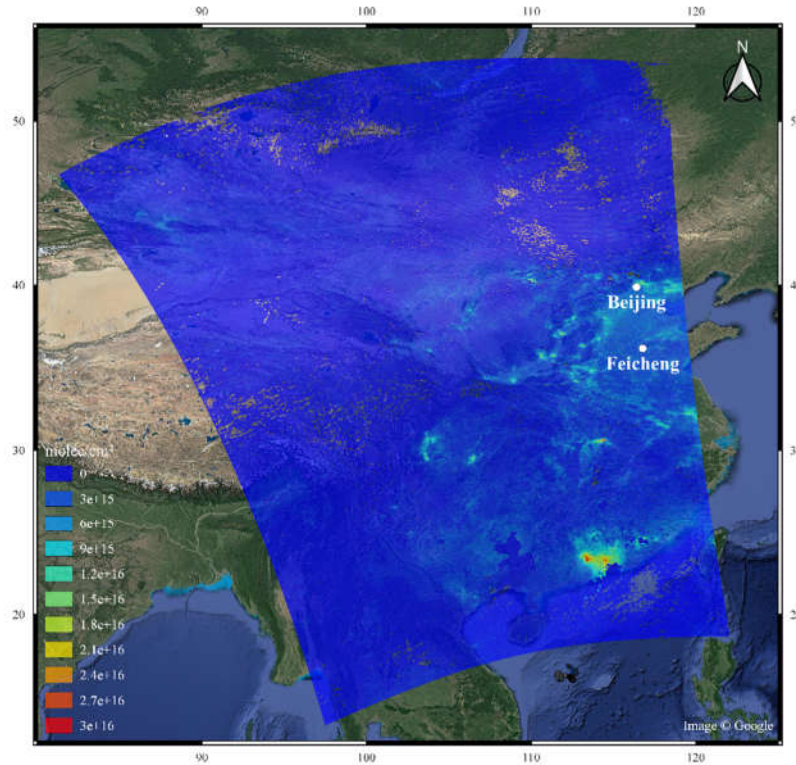
Figure 3. TROPOMI observation of tropospheric NO₂ over China on 23 June, 2018. The location of UVHIS flight (Feicheng city) is also plotted in the map.

9. The authors use a wavelength range between 430 and 470 nm for the DOAS analysis including the cross sections of NO2, O3 and O4, as well as the ring cross section. However water vapour also shows some strong absorption lines in the respective wavelength range (Hitran data base, Rothman 2013), this is not included in the DOAS fit. (see general comment)

We recalculated the NO_2 dSCD by adding a H_2O vapor cross section from HITRAN database. The DOAS fit results and the errors both decreased slightly. For the fit example in the manuscript, the dSCD decreased from $5.05 \pm 0.38 \times 10^{16}$ molec cm^{-2} to $4.95 \pm 0.34 \times 10^{16}$ molec cm^{-2}, while the RMS decreased from 4.56×10^{-3} to 4.27×10^{-3}. We also updated the DOAS fit example figure.
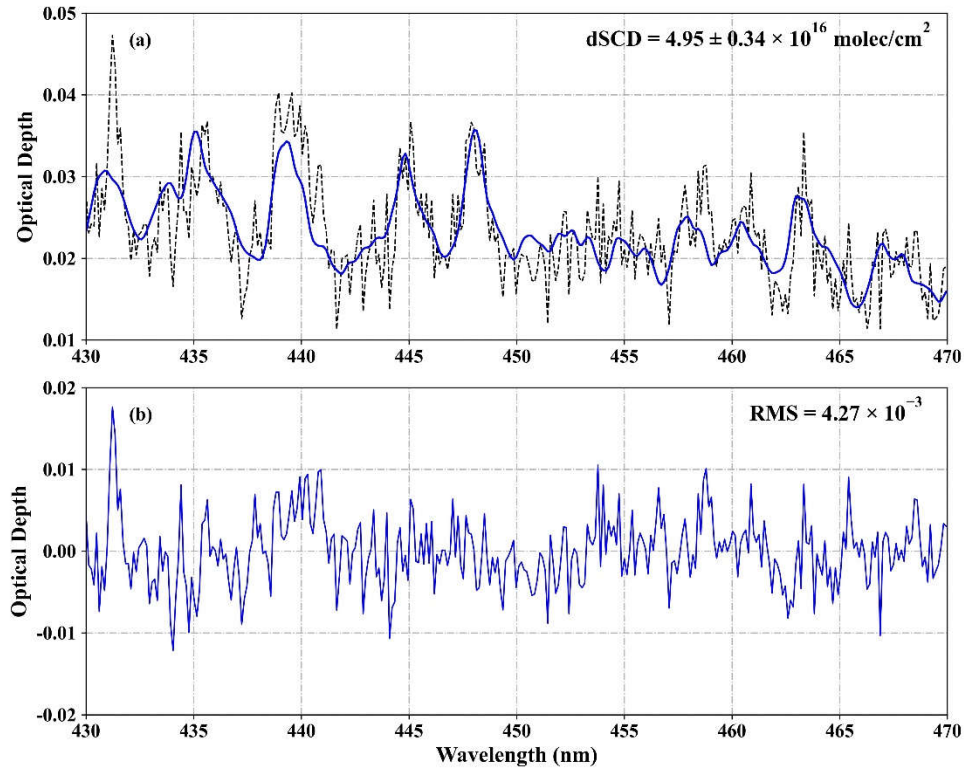
Figure 6. Sample DOAS fit result for NO₂: (**a**) observed (black dashed line) and fitted (blue line) optical depths from measured spectra; (**b**) the remaining residuals of DOAS fit.

10. The tropospheric background of 1 x 10ˆ15 molec/cm^2 as given by Popp et al. (2012) refers to the background around Zürich I am not sure this can be assumed for China as well. Here a satellite observation of the rural background around Feiching might help to estimate a realistic background.

We agree that a satellite observation of the rural area around Feicheng would be a more realistic background estimation. We modified the tropospheric NO₂ vertical column of reference spectra to 3×10^{15} molec cm^{-2} with error of 1×10^{15} molec cm^{-2} based on TROPOMI NO₂ product on the same day. We also updated the UVHIS NO₂ distribution map.
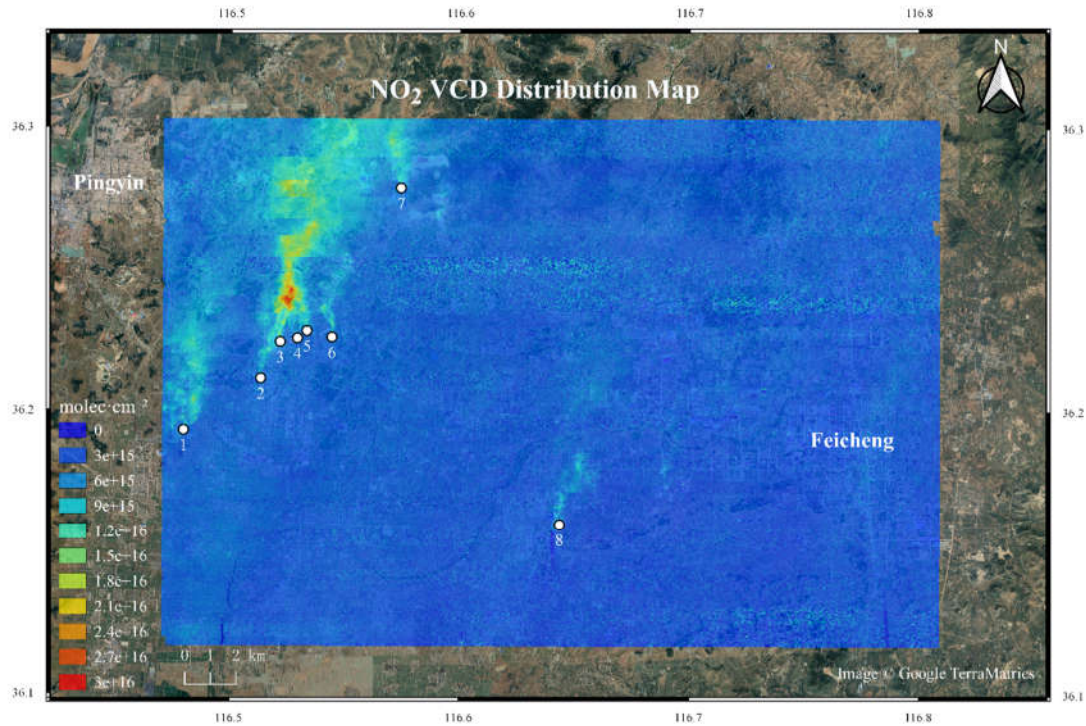
Figure 10. Tropospheric NO$_2$ VCD map retrieved from UVHIS over Feicheng on 23 June 2018. The major contributing NO$_2$ emission sources are indicated by number 1 to 8.

11. The section about the Landsat 8 data analysis and resolution might be shifted from section 4.3.2 to 4.3.1. Meier et al. 2017 developed a method to retrieve the albedo from the measurements did you consider applying a similar method?

We shifted the section about the Landsat 8 data analysis and resolution from section 4.3.2 to 4.3.1. We realize that Meier et al. (2017) developed a method to retrieve surface reflectance from an instrument which is not radiometrically calibrated. However, surface reflectance algorithm for UVHIS is still under development and needs to be verified. We will include this in future works.

12. The assumption about the aerosol optical density, SSA and scattering function are partly given but not justified, the details about the optical density are not given directly.

MODIS AOD product used in this paper is MYD04 on 23 June, 2018, with resampling for every ground UVHIS pixel. The SSA and asymmetry factor of aerosol used in the manuscript are estimation of typical urban/industrial aerosol based on previous studies (Li et al., 2018).

(5) Aerosol optical Depth (AOD) information used in AMF calculation is MODIS AOD product MYD04 at 470 nm on the same day with resampling for every ground UVHIS pixel (Remer et al., 2005), because neither ground-based aerosol measurement is performed, nor any AERONET station data near the flight area is are available. Like the NO_2 profile, the aerosol extinction box profile is constructed from the PBL height and AOD. Single scattering albedo (SSA) is assumed to be 0.93, and asymmetry factor is assumed to be 0.68 for aerosol extinction profile, based on previous studies of typical urban/industrial aerosols (Li et al., 2018).

13. During ascent and decent of the plane you can often estimate the PBL height from visibility or if available dew point measurements. This might be more realistic than the typical summer day assumption of 2000 m. However, the measurements were performed 2 years ago the respective information might be lost. The error is less than 13%, assuming that the PBL reached at least up to 1000 m.

The PBL height was not measured during the flight on 23 June, 2018. Unfortunately, other respective information about PBL height was not available at present.

14. The measurements by Tack et al. (2017) were performed in an SZA range of 40 to 60 degree; in this range the effect of the SZA might be different as in the range between 10 and 40 degree.

We added an AMF dependency analysis on the VZAs, also a new panel in Figure 8. As shown in Fig. 8 (b) and (c), the changes of AMF are 10% and 7% respectively, when other parameters are set as mean.
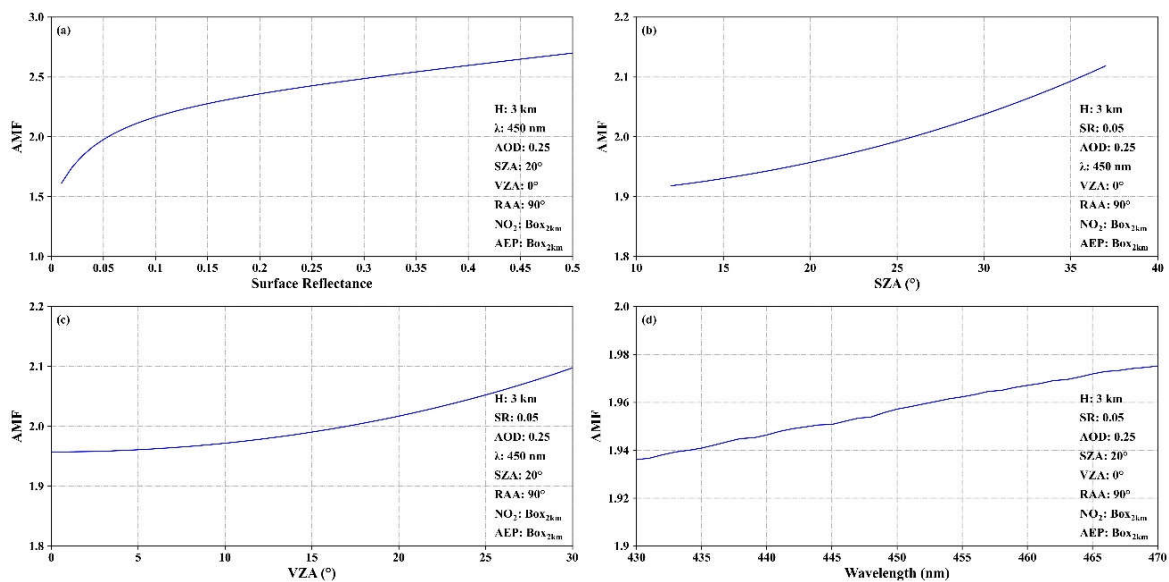
As can be seen in Fig. 7, the effect of sun and viewing geometries on AMFs is very small. Based on a previous study from Tack et al. (2017), changing SZA have the greatest effect on AMFs, in comparison to other sun and viewing geometries. In this study, we also did an AMF dependence analysis on SZAs and VZAs. The SZA varies from 12.8° to 37.4° during the 3 hour research flight, while the VZA ranges from 0° to 30° in most cases. As shown in Fig. 8 (b) and (c), the changes of AMF are less than 10% and 7% respectively, when other parameters are set as mean. Generally, a larger SZA or a larger VZA could result a longer light path through the atmosphere and thus a larger AMF.

15. The uncertainty of the cross section is usually dominated by systematic uncertainty and not by the random errors. Only the random part is included in the QDOAS error analysis.

We agree that the uncertainty of the cross section is usually dominated by systematic uncertainty. We added the word 'systematic' in this sentence.

16. For the reference region a vertical column of 1 x10 ˆ15 molec/cmˆ2 is assumed, therefore for the error of the slant column it should be multiplied by the respective AMF.

We modified the tropospheric NO_2 vertical column of reference spectra to 3×10^{15} molec cm^{-2} with error of 1×10^{15} molec cm^{-2} based on TROPOMI NO_2 product. Also, we fix this error in the calculation of error budget. The mean total value of error is 3.0×10^{15} molec cm^{-2} with a range from 1.5 to 5.9×10^{15} molec cm^{-2}.

The second uncertainty source, σ_{SCDref}, is caused by the NO_2 residual amount in the reference spectra. Since we use TROPOMI tropospheric NO_2 product of the clean reference area as background amount, the uncertainty of NO_2 vertical column is estimated to be 1×10^{15} molec cm^{-2} directly from TROPOMI product. Assuming a tropospheric AMF of 2.0 and a tropospheric AMF over the reference spectra of 1.8, this results an uncertainty 9×10^{14} molec cm^{-2} to the tropospheric vertical column.

17. The focus of the paper is on the airborne instrument. A proper reference to the mobile DOAS instrument should be given, if this is not possible it might worth adding some additional information. Is the tropospheric or the total NO2 column retrieved? How large are the uncertainties of the mobile instrument? Are the same AMF settings (albedo, PBL height, aerosols) used as for the airborne observation?

We added two paragraphs in Sect 6.2 to describe the mobile DOAS tropospheric NO$_2$ retrieval method and its uncertainty analysis. For better comparison with UVHIS NO$_2$ observations, assumptions and parameters in NO$_2$ retrieval method for the mobile DOAS were set to the same as the UVHIS.

For better comparison with UVHIS NO$_2$ observations, assumptions and parameters in NO$_2$ retrieval method for the mobile DOAS were set to the same as the UVHIS. For example, residual amount of NO$_2$ in reference spectra was set to 3×10^{15} molec cm^{-2} with an error of 1×10^{15} molec cm^{-2}; mobile DOAS observations only focus on tropospheric portion of NO$_2$ columns, assumed that the difference of the stratospheric NO$_2$ columns between observed spectra and reference spectra is negligible; vertical profiles of NO$_2$ and aerosol extinction, albedo, and aerosol properties in the AMF calculation were set to the same as UVHIS.

Like the uncertainty analysis of UVHIS NO$_2$ columns, the total uncertainty on the retrieved mobile tropospheric VCD is composed of three parts: (1) the mean uncertainty on dSCD of mobile DOAS is 1.4×10^{15} molec cm^{-2}; (2) the uncertainty of reference vertical column is estimated to be 1×10^{15} molec cm^{-2}. In the case that the tropospheric AMFs of measured and reference spectra are very close, this part results an uncertainty 1×10^{15} molec cm^{-2} to the total uncertainty; (3) the mean relative uncertainty on the AMF calculation is 22 % by square root of the quadratic sum of individual uncertainties like UVHIS. Combining these uncertainties together, the mean total uncertainties on the retrieved tropospheric NO$_2$ VCDs is 2.1×10^{15} molec cm^{-2}.

18. Please add an approximate scale in figure 2 or write some comparable information in the caption e.g. the measurement area was ~20 x 30 km and the distances between parallel lines were 1.5 km In figure 10 the individual sources are numbered it might help to add the numbers already in figure 2 in addition to the description.
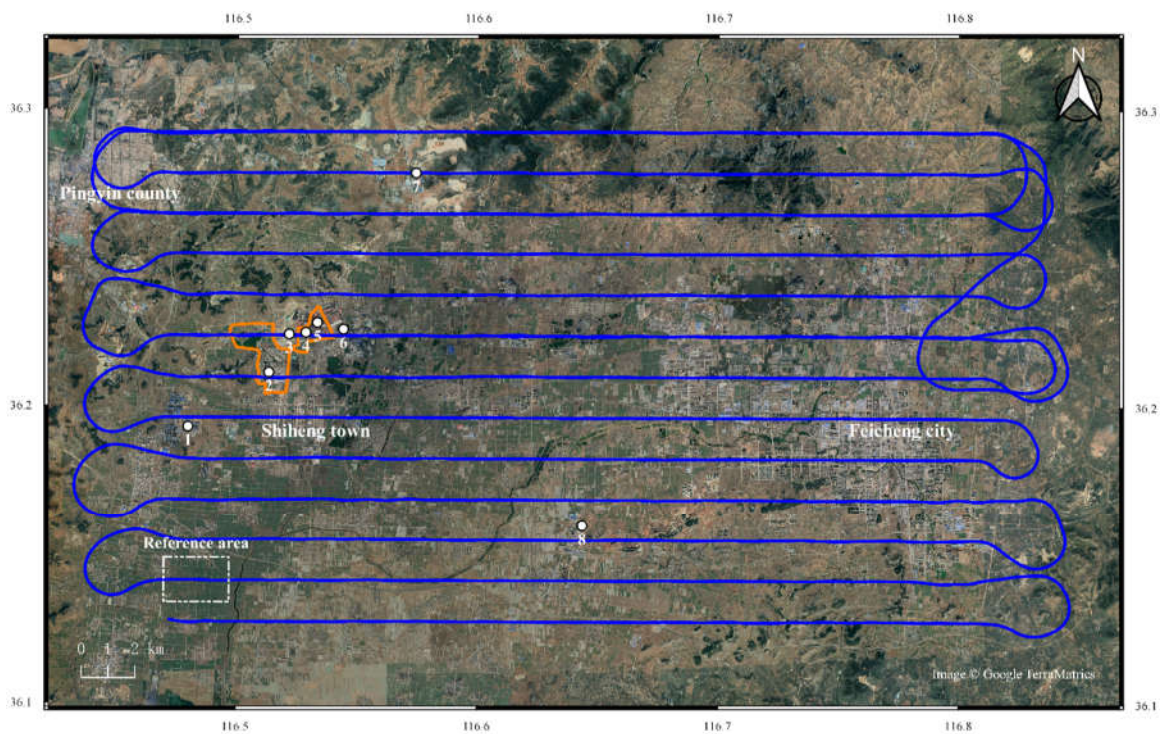
We updated this figure as below:

Figure 4. Overview of the Feicheng demonstration flight on 23 June, 2018. Flight lines are shown in blue. Two orange circles represent the routes of mobile DOAS system. White dots numbered from 1 to 8 represent the major emission sources. Number 1: several carbon factories; number 2: a power plant; number 3-6: individual emitters inside the steel factories, while number 4 and 5 are inside the circle of one mobile DOAS route; number 7-8: two cement factories. White dashed box represents the reference area.

19. L 130: replace one "across track" by "along track"

Corrected.

20. L 163: delete the last sentence starting with "the direct output..." this already written in l 152.

Corrected.

21. L 226: Is [28] a reference? Please use the AMT reference style.

Corrected.

22. L 320: "are near downwind of several plumes" replace by "inside the plumes" or "down-wind of the sources"

Corrected.

23. Figure 8: "wavelength 20 nm" looks like a copy-paste-error from figure 9 "SZA 20◦"?

We consolidated Figures 6, 8, and 9 into new Fgure 8, also we corrected this error.

24. Figures 10 and 11: please add the approximate position of the figure 11 in figure 10 and use the same numbers in figure 11.

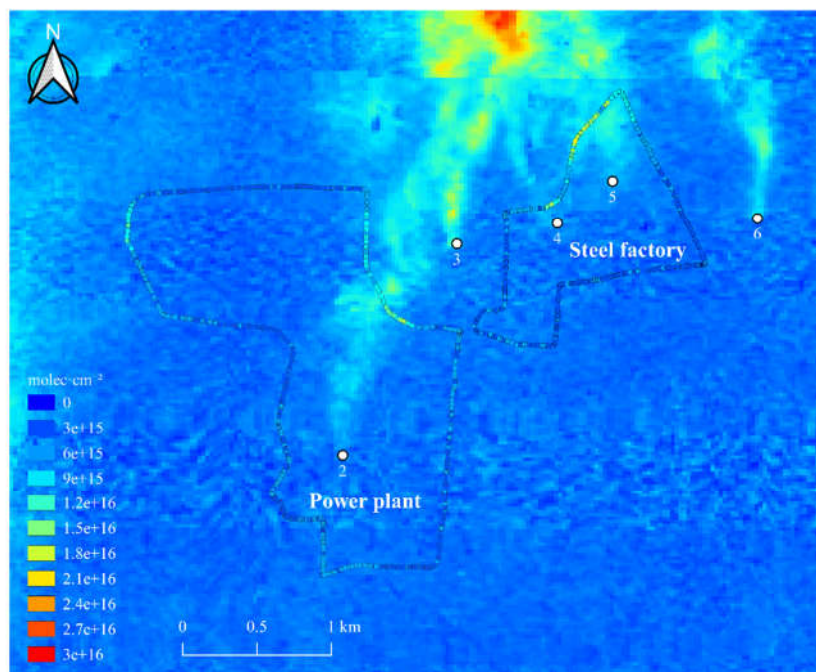We updated Figure 11 with same numbers as below:

Figure 13. Overview of VCDs retrieved from ground-based mobile DOAS system (circle marks), and VCDs retrieved by UVHIS (background layer), measured on 23 June 2018.

25. In some references there is a layout problem with subscripts like in NO2.

Corrected.